Hindawi Publishing Corporation
International Journal of Rotating Machinery
Volume 2013, Article ID 725268, 17 pages
http://dx.doi.org/10.1155/2013/725268

Research Article

Evaluation of the Thermal Effects in Tilting Pad Bearing

G. B. Daniel and K. L. Cavalca

Department of Mechanical Design, Laboratory of Rotating Machinery, Faculty of Mechanical Engineering, University of Campinas, Campinas 13083-970, SP, Brazil

Correspondence should be addressed to K. L. Cavalca; katia@fem.unicamp.br

Received 1 July 2013; Accepted 7 September 2013

Academic Editor: Masaru Ishizuka

The analysis of thermal effects is of expressive importance in the context of rotordynamics to evaluate the behavior of hydrodynamic bearings because these effects can influence their dynamic characteristics under specific operational conditions. For this reason, a thermohydrodynamic model is developed in this work, in which the pressure distribution in the oil film and the temperature distribution are calculated together. From the pressure distribution, the velocity distribution field is determined, as well as the viscous dissipation, and consequently, the temperature distribution. The finite volume method is applied to solve the Reynolds equation and the energy equation in the thermohydrodynamic model (THD). The results show that the temperature is higher as the rotational speed increases due to the shear rate of the oil film. The maximum temperature in the bearing occurs in the overloaded pad, near the outlet boundary. The experimental tests were performed in a tilting pad journal bearing operating in a steam turbine to validate the model. The comparison between the experimental and numerical results provides a good correlation. The thermohydrodynamic lubrication developed in this assignment is promising to consistently evaluate the behavior of the tilting pad journal bearing operating in relatively high rotational speeds.

1. Introduction

Aiming to increase profits and improving economic growth, the industries have been seeking for some ways to raise productivity, such as new technologies, system optimization, and consequently, power source increasing. Those factors allow the machines operation in higher speed accelerating the production system. However, the increment of the operational speed, specifically in rotating machinery, is not a simple task, because it can cause serious problems like affecting the safe operational conditions of the machines. The rotation speed increase in rotating machines can completely change its dynamic behavior, turning an initially stable machine into an unstable one. It mainly occurs due to the dynamic characteristics of the bearing, which tends to change significantly with the rotational speed. One of the reasons is the influence of thermal effects in high rotational speed, because of the shear rate in the oil film, increasing consequently the temperature of the lubricant as well. Therefore, special attention must be taken due to the influence of the thermal effects in the hydrodynamic bearings under certain operational conditions.

An article of valuable contribution to the development of thermohydrodynamic analysis in bearings was published by Dowson in 1962 [1]. In this work, the generalized Reynolds equation was presented, which considers the variation of viscosity and density of the fluid film, both in the radial direction as well as in circumferential and axial directions. From this work, it was possible to accomplish more accurate thermal analysis in hydrodynamic bearings.

Four years later, Dowson et al. [2] developed a thermohydrodynamic analysis by solving the generalized Reynolds equation, the energy and the conduction equations. This analysis was performed as two-dimensional taking into account the properties variation of the lubricant in the circumferential and radial coordinates. Besides, the good agreement of this analysis with experimental results showed that the shaft can be regarded isothermal. Moreover, the temperature gradients in the axial direction can be neglected, since these gradients were very small when compared to the radial and circumferential directions.

In 1975, Hall and Neal [3] analyzed the influence of the effect of different fluid film temperature boundary conditions

on the performance of lubricated bearings. The work pointed out the importance of the boundary temperatures in the bearing behavior. The results showed that the assumption of nonconducting film boundaries do not necessarily lead to a lower boundary solution and the bearing performance is adversely affected by a runner surface temperature higher than the fluid inlet temperature.

In addition to the cylindrical journal bearings, the thermohydrodynamic analysis began to be applied to multilobe bearings, such as two-lobe journal bearing. Nagaraju et al. [4] presented a thermohydrodynamic solution of a finite two-lobe journal bearing. In this analysis, the static characteristics and the dynamic characteristics are evaluated. The results showed that the eccentricity ratio increases and the load capacity decreases with the increasing of the thermal parameter. Moreover, the damped frequency of whirl decreases with the increasing of the thermoviscous coefficient for any load.

From the 1990s many researchers focused their studies on the development of models and analysis of tilting pad journal bearings. In 1990, Taniguchi et al. [5] accomplished a thermohydrodynamic analysis of a tilting pad journal bearing for steam turbines. The three-dimensional thermohydrodynamic analysis presented in this work took into account the laminar and turbulent flow regimes and the mixing temperature in the pad inlet. The numerical results obtained in the simulations presented a good accordance with the experimental data for bearing surface temperatures, frictional losses, and minimum film thickness.

In 1992, Fillon et al. [6] experimentally investigated the influence of the operational conditions in a tilting pad journal bearing. In this assignment, the temperature distribution, pressure distribution, and the film thickness were analyzed for different values of rotational speed, applied load as well as geometric preload in the bearing. The measurements obtained in the tests showed that the operational conditions have a great influence on bearing temperatures, being the rotational speed more influential than the applied load.

An other important article was published by Ha et al. in 1995 [7]. In this work, the effects of the inlet pressure on the thermohydrodynamic performance of a tilting pad journal bearing were evaluated. The numerical results were obtained from the three-dimensional thermohydrodynamic model, taking into account the inlet pressure and the variation of oil viscosity. The bearing characteristics predictions by thermohydrodynamic theory with the inlet pressure were in a good agreement with the experimental results. Furthermore, the results showed that the inlet pressure increases not only the film pressure and the load capacity but also the supply flow rate while decreasing the mixing and bearing surface temperature.

In the same year, Gadangi and Palazzolo [8] studied the transient response of a spinning shaft supported by tilting pad journal bearings with effects of pad flexibility and fluid film temperature. The results obtained in this work showed that the thermal effects had lower influence on the orbit and the minimum film thickness than the effects of the pad deformations. It was also observed that the pressure distribution on the bearing increases when the effects of pad flexibility and fluid film temperature are considered, due to the decreasing of the minimum film thickness.

In order to rapidly determine the maximum temperature, without any numerical programming, Fillon and Khonsari [9] proposed in 1996 a generalized thermohydrodynamic model for tilting pad journal bearings, in which two parameters of temperature rising are defined, allowing the direct evaluation of maximum and average dimensionless temperature of a tilting pad journal bearing. The results obtained through the proposed model were compared with results obtained from classic thermohydrodynamic model and experimental data. Despite the discrepancies, the approached model can be used for a first estimation of the bearing thermal behavior.

Also in this year, Bouard et al. [10] analyzed different turbulent models for thermohydrodynamic analysis in tilting pad journal bearings. The numerical studies accomplished in this work were developed using the finite difference method. The results showed that thermal effects are important to describe the bearing characteristics. At high rotation, significant differences in the pressure peak and temperature distributions were obtained when comparing the laminar and turbulent models.

In 2000, Tanaka [11] published a state-of-art report about thermohydrodynamic analyses and design of journal and thrust bearings. In this report, the main papers, since the publication of the generalized Reynolds equation by Dowson until the recent works that describe advanced models to thermohydrodynamic analyses, were presented. It was possible to follow the evolution of the methodology and the inclusion of the thermal and turbulent effects over the years.

A thermoelastohydrodynamic model to investigate the static performance of tilting pad journal bearings was proposed by Chang et al. in 2002 [12]. In this model, the Newton-Raphson method is employed to obtain the hydrodynamic pressure, the eccentricity, and the pad attitude angles simultaneously. The temperature evaluation is calculated solving the three-dimensional energy equation jointly with the heat transfer equation. The results obtained in this work showed that the influence of the thermal effect in the bearing plays an important role for a good estimation of the bearing behavior.

In order to verify the influence of the thermal effects of the bearing on the dynamic behavior of the rotor, some researchers have analyzed the stability condition of the rotor-bearing system. In 2008, Morton [13] accomplished a review of the investigations over unstable synchronous vibrations in rotating machines, concluding that this behavior can be caused due to thermal variations in the shaft near the bearings and seals.

The leading edge groove (LEG) lubrication technology has revolutionized the hydrodynamic bearing allowing better lubrication conditions and reducing the starvation. In 2010, Bang et al. [14] compared the power loss and the temperature characteristics between LEG tilting pad journal bearings and conventional tilting pad journal bearings with and without a seal tooth.

The experimental results showed that the journal bearings without seal tooth had lower power loss and lower pad temperature than those of journal bearings with seal

tooth. Furthermore, the tests without it showed that the conventional journal bearing was more effective than the LEG journal bearing to decrease power loss and pad temperature.

A new review of the theory applied in the tilting pad journal bearing was published by Dimond et al. in 2011 [15]. In this paper, a theoretical basis for static and dynamic operation of tilting pad journal bearings, over the last 50 years, was presented. The paper showed the development of thermohydrodynamic, thermoelastohydrodynamic, and bulk-flow analyses, discussing the future trends and proposing paths for experimental verification.

As seen in previous studies, the determination of the thermal conditions in tilting pad bearings is very important and of recent interest, due to the influence of these effects in the bearing behavior, and consequently, in the stability conditions of the machine. So, analyses to improve the prediction accuracy of the temperature in the oil film of tilting pad bearings are still an open research topic. In this context, this study aims to evaluate the temperature distribution of a tilting pad journal bearing for steam turbines through a two-dimensional model using the finite volume method. The experimental results obtained from the tests are compared with numerical results, giving an initial good approaching. The thermohydrodynamic model used in this work was developed from the generalized Reynolds equation and energy equation, also considering the mixing temperature distribution in the pad inlet. The improvement in the lubricant temperature estimation can lead to a better approach for the hydrodynamic forces and, consequently, for the dynamic coefficients evaluation as well as for the stability analysis of the whole rotating system.

2. Methodology

The basis of the hydrodynamic lubrication is the theory developed by Reynolds in 1886 [16].

The pressure distribution acting in the oil film of the bearing can be obtained from the solution of the Reynolds equation. However,the classical Reynolds equation was developed taking into account the lubricant oil as isoviscous and incompressible, becoming unfeasible to application in thermohydrodynamic analyses. In order to obtain a more generalized equation, Dowson [1] extended the classical Reynolds equation, including the variation of the density and viscosity in the oil film. The generalized Reynolds equation is presented by

$$\begin{aligned}
&\frac{\partial}{\partial x}\left[(F_2+G_1)\cdot\frac{\partial P}{\partial x}\right]+\frac{\partial}{\partial z}\left[(F_2+G_1)\cdot\frac{\partial P}{\partial z}\right]\\
&\quad=h\cdot\left[\frac{\partial(\rho\cdot U)_2}{\partial x}+\frac{\partial(\rho\cdot W)_2}{\partial z}\right]\\
&\qquad-\frac{\partial}{\partial x}\left[\frac{(U_2-U_1)\cdot(F_3+G_2)}{F_0}+U_1\cdot G_3\right]\\
&\qquad-\frac{\partial}{\partial z}\left[\frac{(W_2-W_1)\cdot(F_3+G_2)}{F_0}+W_1\cdot G_3\right]\\
&\qquad+\int_0^h\left(\frac{\partial\rho}{\partial t}\right)dy+(\rho\cdot v)_2+(\rho\cdot v)_1,
\end{aligned}\tag{1}$$

where

$$\begin{aligned}
F_0&=\int_0^h\frac{1}{\mu}dy,\\
F_1&=\int_0^h\frac{y}{\mu}dy=\overline{y}\cdot F_0,\\
F_2&=\int_0^h\frac{\rho\cdot y}{\mu}(y-\overline{y})\,dy,\\
F_3&=\int_0^h\frac{\rho\cdot y}{\mu}dy,\\
G_1&=\int_0^h\left[y\frac{\partial\rho}{\partial y}\left(\int_0^y\frac{y}{\mu}dy-\overline{y}\cdot\int_0^y\frac{1}{\mu}dy\right)\right]dy,\\
G_2&=\int_0^h\left[y\frac{\partial\rho}{\partial y}\int_0^y\frac{1}{\mu}dy\right]dy,\\
G_3&=\int_0^h y\frac{\partial\rho}{\partial y}dy.
\end{aligned}\tag{2}$$

$P(x,z)$ is the pressure distribution in the lubricant oil, x and z are the circumferential and radial coordinates, respectively, μ is the absolute viscosity of the lubricant oil, ρ is the density of the lubricant oil, h is the thickness of the oil film, W, U and v are the velocity components in the axial, circumferential, and radial direction, respectively, and F_n and G_n are the functions that depend on the viscosity and density, respectively. The subscripts 1 and 2 presented in the velocity components (W, U) refer to the surfaces of the bodies 1 and 2; in this case, the body 1 represents the shaft and the body 2 represents the bearing.

Considering only the variation of viscosity in the oil and steady-state condition, the generalized Reynolds equation is reduced to (3), which is applied in the thermohydrodynamic approach of lubricated bearings

$$\frac{\partial}{\partial x}\left(F_2\frac{\partial P}{\partial x}\right)+\frac{\partial}{\partial z}\left(F_2\frac{\partial P}{\partial z}\right)=\rho\cdot U\cdot\frac{\partial}{\partial x}\left(h-\frac{F_1}{F_0}\right).\tag{3}$$

The thickness of the oil for each pad of the bearing can be obtained from geometric parameters, eccentricity of the shaft, and angular displacement of the pad [17]:

$$\begin{aligned}
h(\beta)=R_P-R_S-\{&\sin(\beta)\cdot[y_S+\alpha\cdot(R_P+h_P)]\\
&+\cos(\beta)\cdot(x_S+R_P-R_S-h_0)\}.
\end{aligned}\tag{4}$$

According to Figure 1, β is the angular position on the pad, R_P is the radius of the pad, R_S is the radius of the shaft, O_P is the center of the pad, O_S is the center of the shaft, h_P is

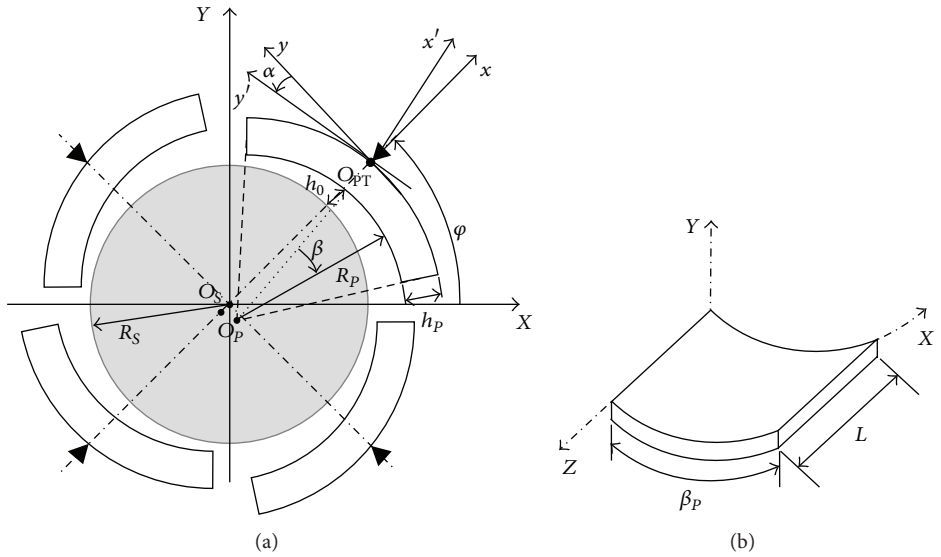

Figure 1: Schematic representation: (a) front view of the rotor bearing; (b) perspective view of the pad.

the thickness of the pad, h_0 is the radial clearance, α is the angular displacement of the pad, and x_S and y_S are the position of the shaft in the local referential system (x,y).

The pressure distribution is iteratively calculated with the temperature distribution. For this reason, the energy equation is applied to determine the temperature distribution in the oil film. In this case, an approach of no heat transfer was considered through the axial coordinate. Based on Cameron [18], this effect can be neglected regarding the radial and circumferential directions of the system. Therefore, the energy equation is given by the following expression [19, 20]:

$$\rho \cdot C_f \cdot \left(u \cdot \frac{\partial T}{\partial x} + v \cdot \frac{\partial T}{\partial y} \right) = k_f \cdot \left(\frac{\partial^2 T}{\partial x^2} + \frac{\partial^2 T}{\partial y^2} \right) + \mu \cdot \Phi, \tag{5}$$

$$\Phi = 2 \cdot \left[\left(\frac{\partial u}{\partial x} \right)^2 + \left(\frac{\partial v}{\partial y} \right)^2 \right] + \left(\frac{\partial u}{\partial x} + \frac{\partial v}{\partial y} \right)^2 + \left(\frac{\partial w}{\partial x} \right)^2 + \left(\frac{\partial w}{\partial y} \right)^2, \tag{6}$$

where $T(x, y)$ is the temperature distribution, k_f is the thermal conductivity, C_f is the specific heat, u, v, and w are the linear velocities in x, y, and z, respectively, and Φ is the viscous dissipation of the oil.

As can be seen in (6), the viscous dissipation is calculated from the velocity components of the lubricant oil. This velocity field in the bearing can be obtained from the Navier-Stokes equation and the continuity equation, as proposed by Dowson [1]. Applying the boundary conditions of the hydrodynamic bearing in the Navier-Stokes equation, the velocities in the axial and circumferential directions can be determined [18]:

$$u = \frac{\partial P}{\partial x} \cdot \int_0^y \frac{y}{\mu} dy + \left(\frac{U}{F_0} - \frac{F_1}{F_0} \cdot \frac{\partial P}{\partial x} \right) \cdot \int_0^y \frac{1}{\mu} dy, \tag{7}$$

$$w = \frac{\partial P}{\partial z} \cdot \int_0^y \frac{y}{\mu} dy - \left(\frac{F_1}{F_0} \cdot \frac{\partial P}{\partial z} \right) \cdot \int_0^y \frac{1}{\mu} dy. \tag{8}$$

From the axial (w) and circumferential (u) velocities and applying the continuity equation, the radial velocity is determined:

$$v = - \int_0^y \left(\frac{\partial u}{\partial x} + \frac{\partial w}{\partial z} \right) dy. \tag{9}$$

Equation (5) gives the temperature distribution in the xy plane (radial and circumferential direction) for different axial positions, such as the central plane and at the edges planes of the bearing. Although no heat conduction is considered through the axial coordinate, the temperature varies in this direction of the bearing due to the pressure distribution variation in the axial direction and, consequently, the velocities field and thermal dissipation as well. In fact, the temperature variation in the axial direction is very low, in compliance with the assumptions that the heat transfer is also very low, leading to neglecting it in this direction, so that the temperature is practically regular. Regarding the boundary conditions, the heat conduction between the fluid and the journal was taken into account, in which the journal was isothermal, and there was no heat transfer between the fluid and the bearing wall (adiabatic condition). These assumptions were adopted from previous studies [2, 21, 22]. Furthermore, the boundary conditions in the inlet and the outlet of the pad were considered as prescribed temperature and adiabatic, respectively. The regarded temperature in the inlet of the pad is the mixing temperature obtained between the flow of

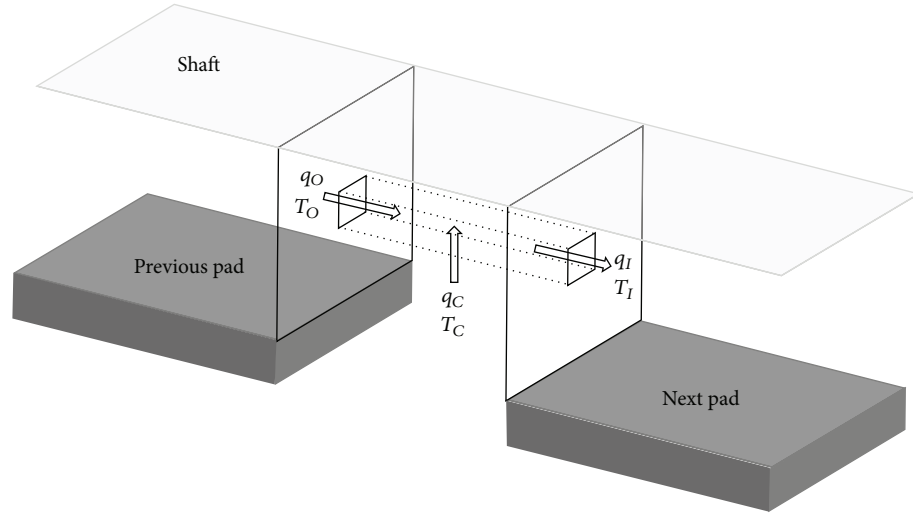

Figure 2: Energy balance in the mixing region between the pads, highlighting one of the control volumes of this region.

the previous pad and the flow of oil supply (cool oil). Due to the rotation of the journal, the oil velocity in the outlet of each pad is high, causing a mixing region in the inlet boundary of next pad. For this reason, no heat transfer occurs in the outlet boundary of the pads, leading to an adiabatic boundary condition.

In this work, the mixing temperature was modeled from the energy balance in the region between pads (mixing region). Control volumes were supposed between the volumes in the outlet of the previous pad and the volumes in the inlet of the next pad. Figure 2 shows the mixing region between pads, highlighting just a single control volume.

According to Figure 2, the energy balance in the control volume can be written as [22]

$$T_I = \frac{T_O \cdot q_O + T_C \cdot q_C}{q_O + q_C}, \tag{10}$$

where T_I is the temperature in the inlet face of a volume located at the inlet boundary of the next pad, T_O is the temperature in the outlet face of a volume located at the outlet boundary of the previous pad, T_C is the temperature of the oil supply (cool oil), and q_C is the flow of the oil supply (cool oil) in each control volume. The temperature of the oil supply is considered uniform for all the mixing region (region between pads), and the total flow of the oil supply in the mixing region (Q_C) is equally distributed among all control volumes, resulting in the flow of oil supply in each control volume (q_C). In practical applications, both the temperature and flow of the oil supply are known, because these parameters are generally measured and controlled in the rotating machines, such as steam turbines and compressors.

The outlet flow of a volume is calculated from the velocity component perpendicular to the area of the outlet face

$$q_O = \int_A u \cdot dA, \tag{11}$$

where A is the area of the outlet face and u is the circumferential velocity component presented in (7).

The approach of the mixing region used in this work represents a new approach of the temperature estimation inside the bearing. Different from standard approaches, the temperature estimated in the mixing region is not a global temperature. According to Figure 2, control volumes are considered in the region between the pads, while the standard approach considers the region between the pads as only one control volume. Therefore, the new approach estimates a temperature distribution for the inlet face of the pad and not only one value (global temperature).

The Reynolds' equation and energy equation are partial differential equations, in which it is not possible to obtain the full analytical solution. For this reason, the use of numerical methods for solving these equations is often employed. In this work, the finite volume method (FVM) is applied to solve the Reynolds equation and the energy equation, as proposed by Maliska [20].

Since the mesh used to solve the temperature distribution is not uniform due to the variation of the film thickness in the circumferential direction, the mesh discretization in this case is not a simple task. To facilitate this process a coordinate transformation is required [20], aiming to transform the nonuniform mesh (physical domain) in a uniform (computational domain) as shown in Figure 3.

As previously described, the numerical method applied to solve the differential equations of this problem (Reynolds equation and energy equation) was the finite volume method (FVM) and the iterative method for solving the linear systems of equations was the Gauss-Seidel method.

The mesh used in the numerical solution was defined by convergence analysis of the problem. After several tests for numerical convergence, the mesh composed of 32 volumes in each direction showed the best performance in terms of computational time and solution convergence, that is, $N_x = 32$, $N_y = 32$, and $N_z = 32$ volumes.

Regarding the boundary conditions, a prescribed temperature was assumed in the oil film in the shaft boundary (shaft temperature) and in the inlet face of each pad (mixing

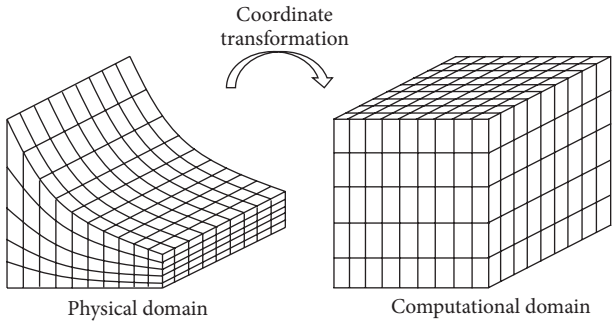

Figure 3: Transformation from physical to computational domain.

region temperature). Moreover, the numerical simulation considered the outlet boundary and the pad surface boundary as adiabatic condition due to the minimum heat transfer occurred in these faces (practically nil). Figure 4 shows a schematic representation with the mesh and the boundary conditions in one pad of the bearing.

3. Experimental Tests

3.1. Description of the Experimental Tests. The experimental results were obtained in a steam turbine during tests performed to ascertain the specifications and requirements of the client.

The test consists in running the steam turbine at its operational speed and monitors the vibration levels of the rotor, oil flow, temperature of the oil supply, and temperature of the oil inside the tilting pad bearing. Attempting to use these experimental results to comparison with the numerical results of the thermohydrodynamic model, the measurements presented in this paper are the flow, the temperature of the oil supply, and the temperature of the oil inside the bearing. However, in order to eliminate the eventual effects of the coupling, the measurements used in this work are related to the bearing of the free extremity of the shaft.

Figure 5 shows the schematic representation of the experimental system used in this work.

According to Figure 5, the temperatures inside the bearings are measured by PT100 sensors (standard platinum thermoresistance) whose resolution is 0.5°C. The measurements are conditioned in a control cabinet and sent to the signals acquisition computer. The hydraulic system is also monitored by the control cabinet, allowing setting the pressure of the pump and controling the oil flow and temperature of the oil supply. The tests performed in this work used a pumping pressure of 2.5 bar, resulting in an oil supply flow of 250 L/min, measured by the flow sensor; that is, the oil supply flow is 125 L/min in each tilting pad bearing. Moreover, a PT100 sensor assembled in the hydraulic line after the pump measures the temperature of the oil supply, at about 45°C.

The operational conditions and the geometric parameters located at the bearing are presented in Table 1.

The temperature of the oil inside the bearing is measured through the temperature sensor PT100. According to Figure 6, this temperature sensor is assembled in a specific position near the pad outlet, close to the region where the lubricant presents its highest temperature. As the outlet pad depends on the rotation of the rotor, the pads generally present two possible positions to assemble the sensors, focusing to attend the operation in both rotation directions (clockwise and counterclockwise). The assembly of these sensors must be accomplished with precision not to restrict in the angular displacement of the pad and, consequently, not to interfere in the equilibrium position of the pad and the shaft inside the bearing.

Table 1: Geometric parameters and operational condition of the bearing.

Parameters/data	Values
Operational speed (rpm)	6000
Number of pads	5
Pad angle (degrees)	60°
Angle between pads (degrees)	12°
Shaft diameter (mm)	179.660 0/−0.020
Pad width (mm)	90.000 −0.072/−0.107
Pad diameter (mm)	180.520 +0.029/0
Pad thickness (mm)	25.000 +0.005/0
Assembly clearance (mm)	0.260
Angular position of the pivots in the bearing (degrees)	18°/90°/162°/234°/306°
Pivot position in the pad	0.5 (Central Pivot)
Bearing configuration	LBP (Load between Pivot)
Load (kN)	21.58
Lubricant oil	ISO VG 46

In the experimental tests presented here, the rotor runs in the counterclockwise direction. For this reason the temperature sensor is assembled in the right side of the pad 5, where the highest values of the temperature in the bearing occur.

Figure 6 shows the position of the pads in the bearing and the position of the sensor in the pad.

3.2. Experimental Results. As previously described, the flow and the temperature of the oil supply are measured during the experimental test, as presented in Figure 7. As can be seen, the temperature of the oil supply is 45°C and its flow is nearly 250 L/min (liter per minute), being equally divided in both bearings; that is, the flow of the oil supply in each bearing is 125 L/min. After tuning the steam turbine conditions, the rotor starts to operate (in standard operation). The rotor starts from the stationary condition, slowly increasing the rotational speed until 6600 rpm, which is 10% greater than its nominal operational speed. Then, the rotor speed is decreased to the operational speed (6000 rpm), remaining in this condition until the end of the measurements.

Figure 8 presents the temperature measured inside the bearing (at pad 5) during the test. It is noticed that when the rotor is in stationary condition, there are no thermal effects in the lubricant fluid, and consequently the temperature measured inside the bearing is the same as found in the oil supply,

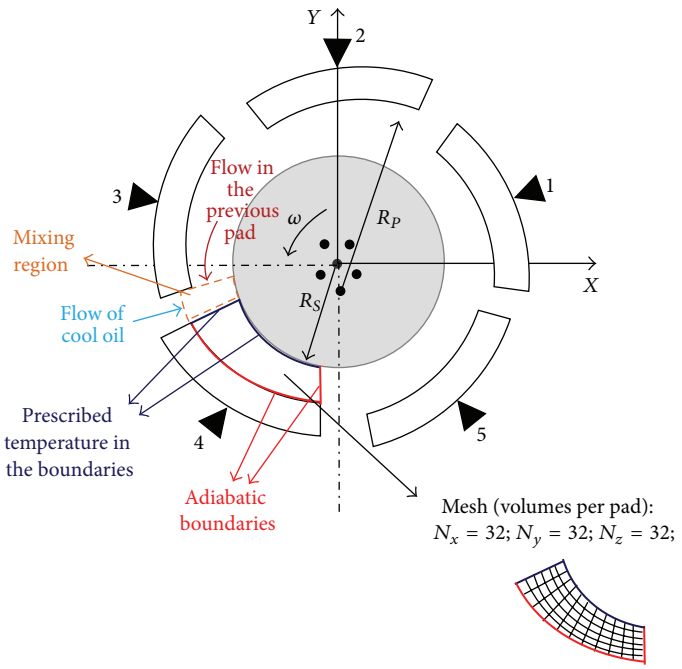

Figure 4: Schematic representation of the mesh and the boundary conditions.

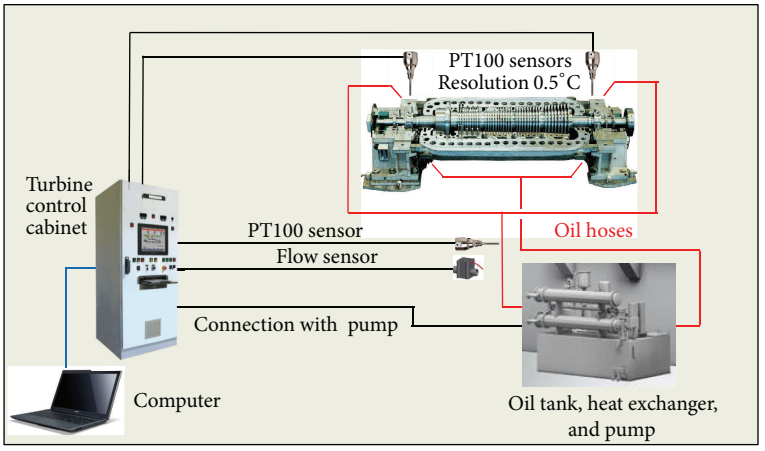

Figure 5: Schematic representation of the experimental system.

that is, about 45°C. However, as the rotor speed increases, the viscous dissipation of the lubricant also increases, resulting in higher values of temperature measured inside the bearing. The maximum temperature measured inside the bearing was about 82°C, occurring when the rotor was running in the maximum rotational speed (6600 rpm). At the operational speed (6000 rpm), the temperature measured inside the bearing is a little bit lower, about 80°C.

4. Numerical Simulations

4.1. Description of the Numerical Procedure. The analysis of thermohydrodynamic problems in lubricated bearings requires the solution of the pressure distribution simultaneously with the temperature distribution. The algorithms used in these analyses are complex routines since many iterative processes are involved, resulting in high computational costs.

Figure 9 shows the general flowchart used in the thermohydrodynamic analysis. The initial temperature distribution is estimated using the boundary conditions considered in the input data. From the estimated temperature distribution and the constitutive equation of the lubricant, the viscosity field in the oil film of the bearing can be evaluated. After that, the pressure distribution is calculated through the generalized Reynolds equation. In this work, the finite volume method (FVM) is used to solve the Reynolds' equation and the convergence of the solution is obtained through the Gauss-Seidel method (iterative process). From the pressure distribution, the velocity fields and the viscous dissipation can be calculated, and then a new temperature distribution

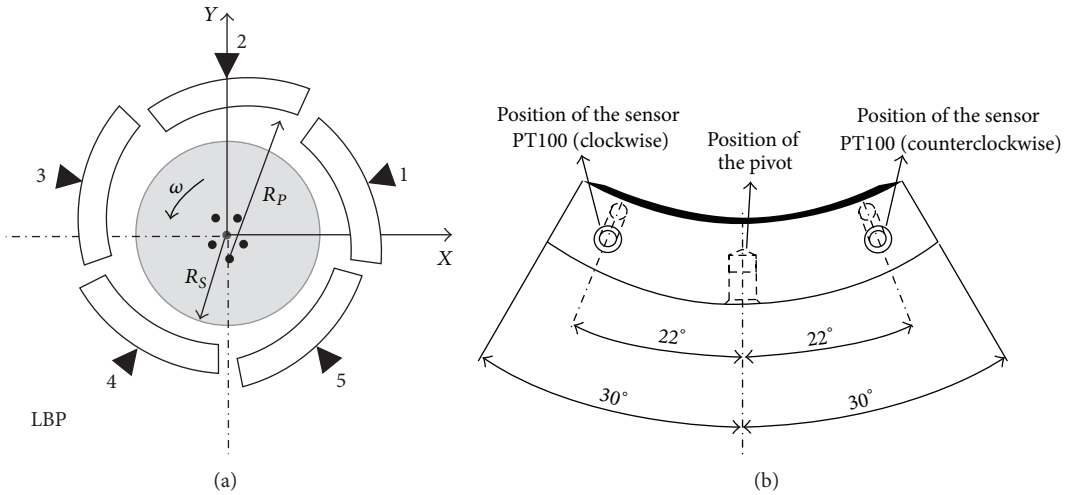

FIGURE 6: Schematic representation of the bearing and the pad: (a) tilting pad bearing with 5 pads; (b) pad of the bearing.

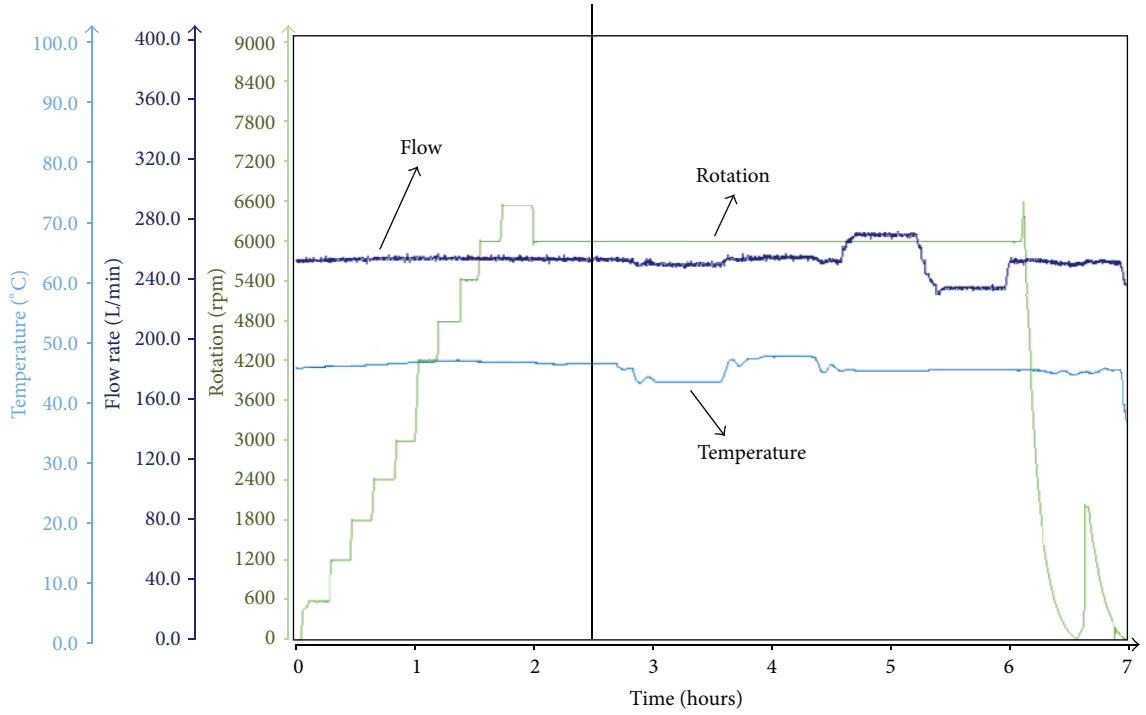

FIGURE 7: Experimental results: temperature of the oil supply; flow rate of the oil supply; rotational speed of the rotor.

is obtained from the energy equation. As considered in the solution of the Reynolds equation, the finite volume method and the Gauss-Seidel method are also used to solve the energy equation. After determining the new temperature distribution the convergence must be verified, by comparing the new temperature distribution with the previously estimated temperature. If the difference between these temperature distributions is lower than the stop criterion, the temperature distribution is converged. However, if the difference is greater, the calculated temperature distribution is assumed as estimated and the calculation process (loop) should be repeated until the convergence.

This general flowchart given in Figure 9 represents the routine used in the thermohydrodynamic analysis of cylindrical and tilting pad bearings. However, this routine cannot be applied independently to each pad of the tilting pad bearing, because the temperature distribution of the previous pad influences the temperature distribution of the next pad. According to Figure 10, there is a mixing region between the pads in which the flow of the previous pad is mixed with the flow of the cool oil before reaching the next pad. Thus, the temperature in the pad inlet (boundary condition) is the temperature obtained in the mixing region due to the flow of the previous pad and the flow of the cool oil. So,

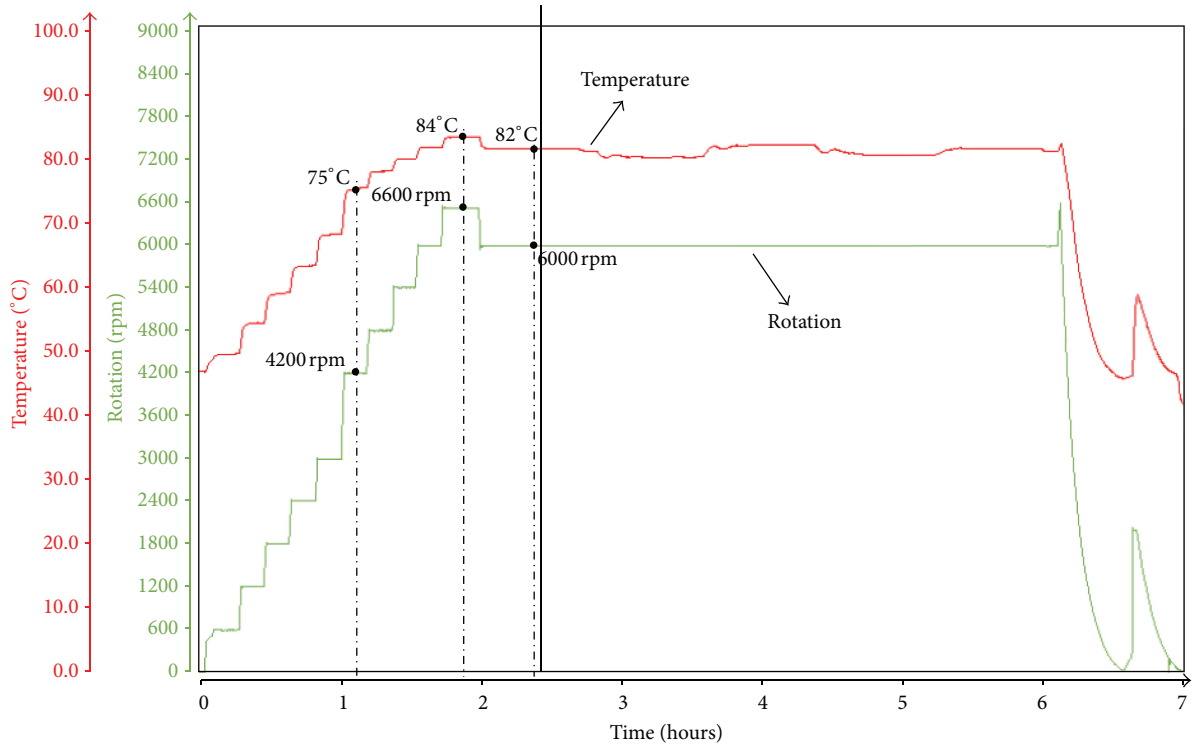

Figure 8: Temperature of the oil measured inside the bearing.

the thermohydrodynamic analysis in the tilting pad bearing is accomplished to each pad of the bearing, taking into account the temperature distribution in the previous pad to calculate the temperature in the pad inlet (mixing region).

4.2. Numerical Results. The boundary condition in the pad outlet (east boundary) is considered adiabatic. There is no heat transfer in this boundary due to the intensity and direction of the oil flow. As previously described in Figure 10, the mixing region occurs near the next pad.

The boundary condition of the pad surface (south boundary) is also considered adiabatic. From this condition, the temperature on the pad surface is calculated and compared with the temperature measured during the test.

The boundary condition in the pad inlet (west boundary) is regarded as prescribed temperature, in which the value of this temperature is due to the mixing of the supply flow and the one of the previous pad. For this reason, it is necessary to know the flow and the temperature of the oil supply. Figure 7 shows the values of the flow (L/min) and the temperature (°C) of the oil supply measured during the test.

The boundary condition of the shaft surface (north boundary) is considered as a prescribed temperature. According to the test standards, the steam turbine was run in low power, in which the value of 50°C represents a good estimation to the temperature of the rotor surface in the bearing region.

As presented in Table 1, the values of the shaft diameter and pad diameter require a tolerance range. For this reason, the radial clearance of the bearing has a maximum and a minimum value. From the data presented in Table 1, the radial clearance can be obtained as $h_0 = R_P - R_S - h_m$, where R_P is the pad radius, R_S is the shaft radius, and h_m is the assembly tolerance, as showed in Figure 11. Thus, the maximum radial clearance is 0.194 mm and the minimum radial clearance is 0.170 mm.

After establishing the boundary conditions, the bearing data and the operational conditions, the computational simulations can determine the pressure distribution and the temperature distribution from the thermohydrodynamic lubrication model. In order to improve the comparison of the numerical and experimental results, the computational simulations were performed to the condition of minimum and maximum radial clearance. Firstly, the results obtained to the condition of minimum radial clearance are presented, and afterwards the results obtained to the condition of maximum radial clearance.

Figure 12 shows the pressure distribution obtained in the maximum rotational speed (6600 rpm) considering the minimum radial clearance in the bearing.

According to Figure 12, the pressure distributions on pads 1 and 3 are similar. Likewise equal pressure distributions can be found on pads 4 and 5. Due to the symmetric distributions obtained on the pads 1 and 3 and on the pads 4 and 5, the resultant force in the X axis on the bearing tends to zero. The resultant force in the Y axis is obtained from the difference between upper and bottom pressure distribution on the pads, with this force being accountable for the rotor supporting.

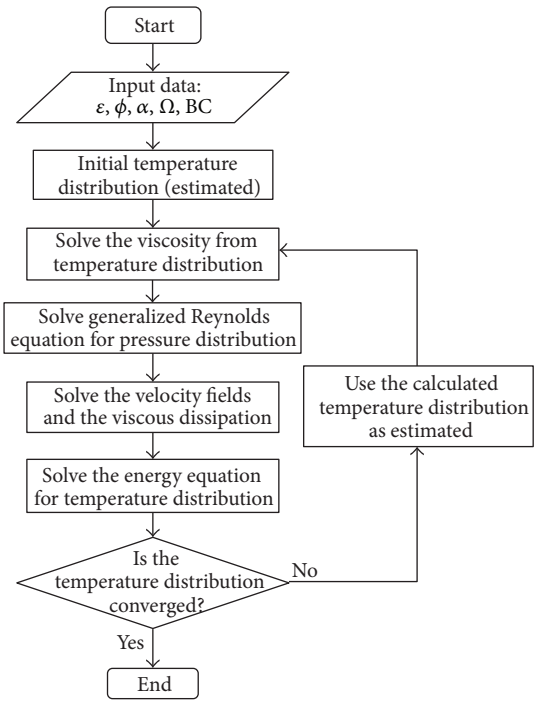

Figure 9: General flowchart of the routine for thermohydrodynamic analyses.

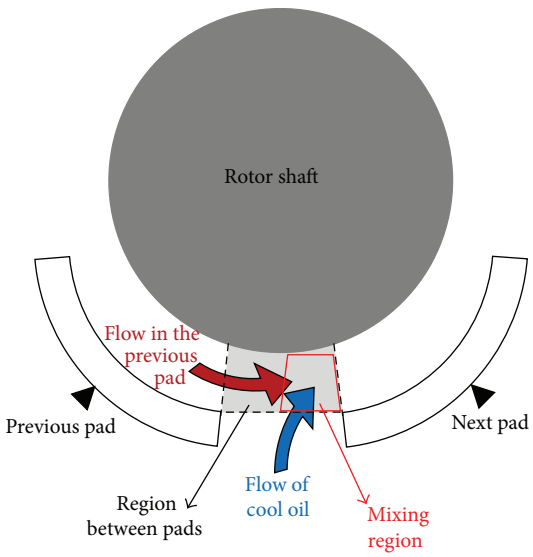

Figure 10: Mixing region between pads in the tilting pad bearings.

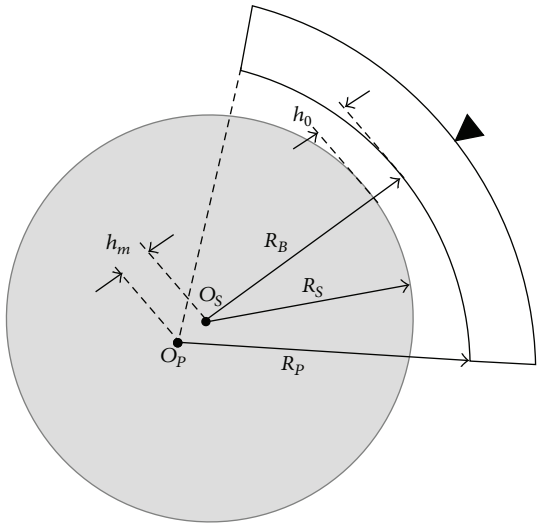

Figure 11: Geometric parameters and clearances in the pad.

Figure 13 shows the temperature distribution obtained in the pads of the bearing when considering the minimum radial clearance. These temperature distributions are obtained in the mid span position of the axial direction. As can be verified in Figure 13, the pads 1 and 3 have approximately the same oil film thickness, resulting in similar temperature distributions. This behavior is also verified in the pads 4 and 5. However, the oil film thicknesses in these pads are lower due to the bearing load, and consequently the temperature values are greater in these pads. Furthermore, it is also possible to verify that the pad 2 has the highest oil film thickness, resulting in a distribution of temperature with the lowest values.

According to Figure 13, it is possible to verify that the temperature distributions have the same behavior in all pads of the bearing. The maximum value occurs in the right inferior corner of the pad, due to the highest shear rate of the lubricant in this position (smallest oil film thickness) and the adiabatic conditions considered on the pad surface and in the pad outlet.

At the inferior left corner of the pad, there is a lower temperature due to the flow of the oil supply. This behavior

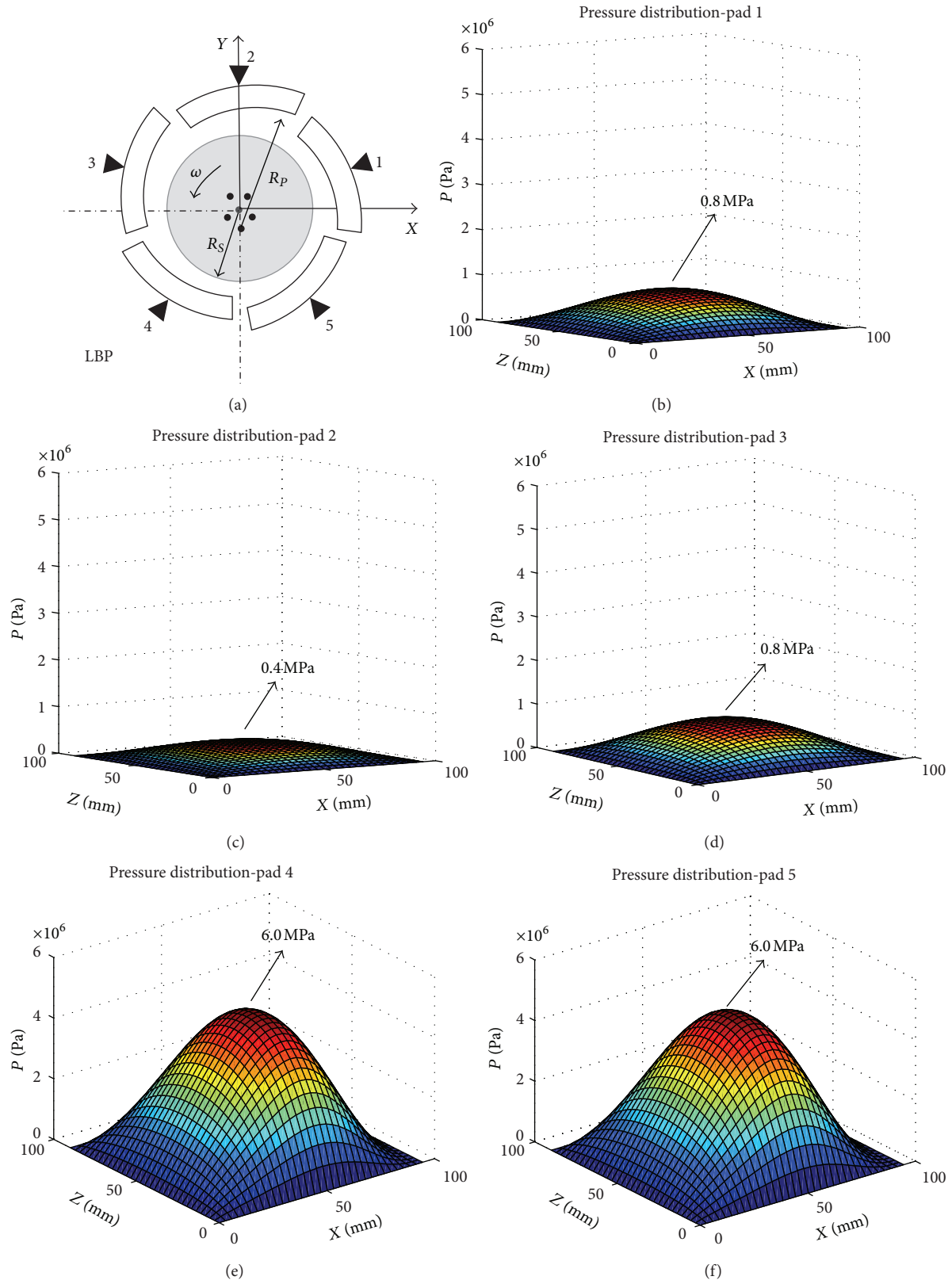

FIGURE 12: Pressure distribution on the pads obtained from the lower radial clearance and the maximum rotational speed: (a) bearing configuration; (b) pad 1; (c) pad 2; (d) pad 3; (e) pad 4; (f) pad 5.

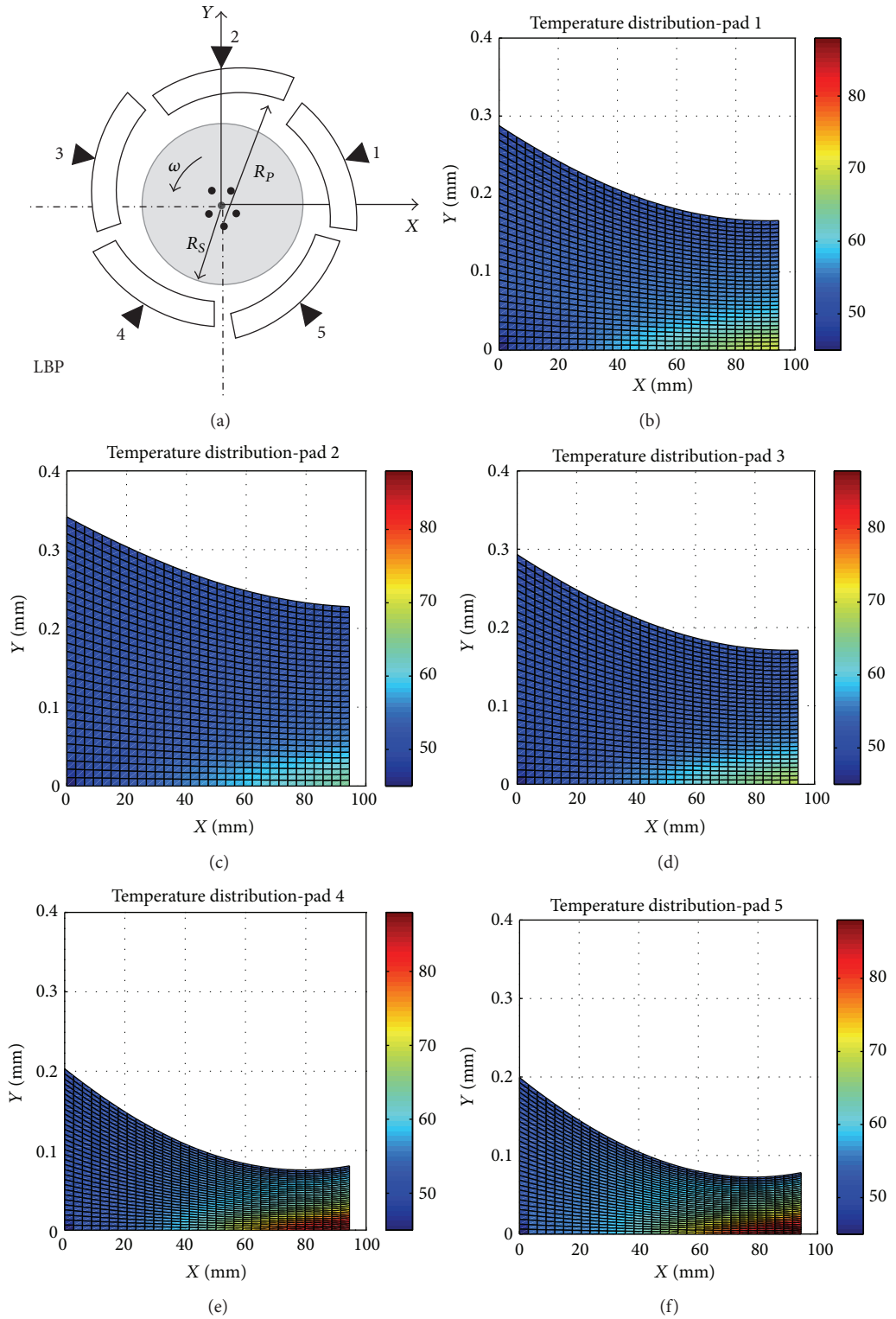

FIGURE 13: Temperature distribution on the pads obtained from the lower radial clearance and the maximum rotational speed: (a) bearing configuration; (b) pad 1; (c) pad 2; (d) pad 3; (e) pad 4; (f) pad 5.

occurs because the flow of the previous pad is practically null in this region; that is, the flow is basically due to the oil supply. Therefore, the oil temperature in this region is about the temperature of the oil supply (45°C).

Figure 14 shows the pressure distribution obtained in the maximum rotational speed (6600 rpm) when considering the maximum radial clearance in the bearing.

Although the general behavior in Figure 14 is similar to that shown in Figure 12, it is possible to verify that the pressure peaks are higher when considering the minimum radial clearance (Figure 12).

Figure 15 shows the temperature distribution obtained in the pads of the bearing for the maximum clearance.

According to Figures 13 and 15, the maximum values of the temperature distribution are obtained on pad 5, leading to calculating the temperature in this pad for the whole range of speed. For this reason, the temperature of the oil inside the bearing is measured in this pad during the experimental tests.

From the results obtained in the computational simulations, the maximum temperature on pad 5 can be determined for a range from 3500 rpm to 6600 rpm. Moreover, it is also possible to evaluate the temperature in the sensor position, which can be compared to the temperature measured in the bearing during the experimental tests.

Figure 16 shows the maximum temperature and the temperature in the sensor position on pad 5.

According to Figure 16, the temperature difference obtained in the conditions of minimum radial clearance and maximum radial clearance tends to be higher as the rotational speed increases. As previously described, the temperature is higher for the minimum radial clearance, because the shear rate and, consequently, the thermal dissipation of the oil film are higher in this condition. So, it is possible to verify that the maximum temperature on pad 5 is slightly higher than the temperature in the sensor position (about 1°C). For example, in the operational rotation (6000 rpm) the maximum temperature obtained is 85°C while the temperature in the sensor position is 84°C.

In order to validate the thermohydrodynamic lubrication model, Figures 8 and 16 should be compared. The numerical results show that the temperatures in the sensor position are about 76°C at 4200 rpm 84°C at 6000 rpm and 86°C at 6600 rpm, while the experimental results show that the measured temperatures are about 75°C at 4200 rpm, 82°C at 6000 rpm, and 84°C at 6600 rpm. The difference between the numerical and the experimental results is about 2°C,which represents a good correlation. However, the numerical results are higher than the experimental ones with this behavior being already expected. The numerical evaluation is more conservative than the real case, due to the adiabatic condition in some boundaries (bearing and pad outlet). As already known, adiabatic condition approach represents a totally null heat transfer, what cannot be true in some practical conditions.

The experimental measurements were accomplished in a real machine during the manufacturer performance tests, and, in this case, the main focus was the temperature control instead of the pressure distribution control. However, the oil film temperature evaluation depends on the equilibrium position of the shaft inside the bearing, which in turn, results from the hydrodynamic forces equilibrium. Finally, the hydrodynamic forces are obtained from the pressure distribution integration in the bearing. At this point, the temperature experimental validation can be considered a good indicative that the equilibrium position and the pressure distribution are consistent with the real behavior of the machine.

5. Conclusion

This assignment presents a contribution to the modeling of tilting pad journal bearings when considering the thermohydrodynamic lubrication condition. Therefore, this work allows evaluating the lubrication conditions and the thermal effects in the bearing.

The results obtained in the computational simulations show that the maximum temperature occurs at the pad outlet, because this region presents the lower film thickness. Such behavior is consistent because the shear rate of the fluid is directly proportional to the gradient of velocity; that is, a smaller film thickness results in greater shear rates and, consequently, greater viscous dissipation. Also for this reason, the pads 4 and 5 present the highest temperature distributions, because these pads are subjected to higher load in smaller film thickness. So it is possible to verify that the maximum temperature in the bearing occurs in pad 5, because the lubricant film thickness is smaller and the temperature received from the previous pad is higher in this pad. An other phenomenon observed in the results is the lower temperature near the pad inlet surface, as a consequence of the mixing between the flow of the oil supply and the flow of the oil inside the previous pad.

The experimental results were obtained from the tests in a real turbine, monitoring the temperature and flow of the oil supply (input conditions) and the temperature of the oil inside the bearing. These experimental results validate the numerical results obtained in the computational simulations. A good correlation is verified between the temperature measured inside the bearing (Figure 6) and the temperature determined from the thermohydrodynamic lubrication model (Figure 13(b)). It is possible to conclude that this lubrication model developed in this work is promising to consistently evaluate the thermohydrodynamic behavior of the tilting pad journal bearing.

Nomenclature List

C_f:	Specific heat of the lubricant oil
F:	Functions that depend on the viscosity
G:	Functions that depend on the density
h:	Thickness of the oil film
h_P:	Thickness of the pad
h_0:	Radial clearance
k_f:	Thermal conductivity of the lubricant oil
P:	Pressure distribution in the lubricant oil
N_x, N_y, N_z:	Number of volumes in X, Y, and Z directions, respectively

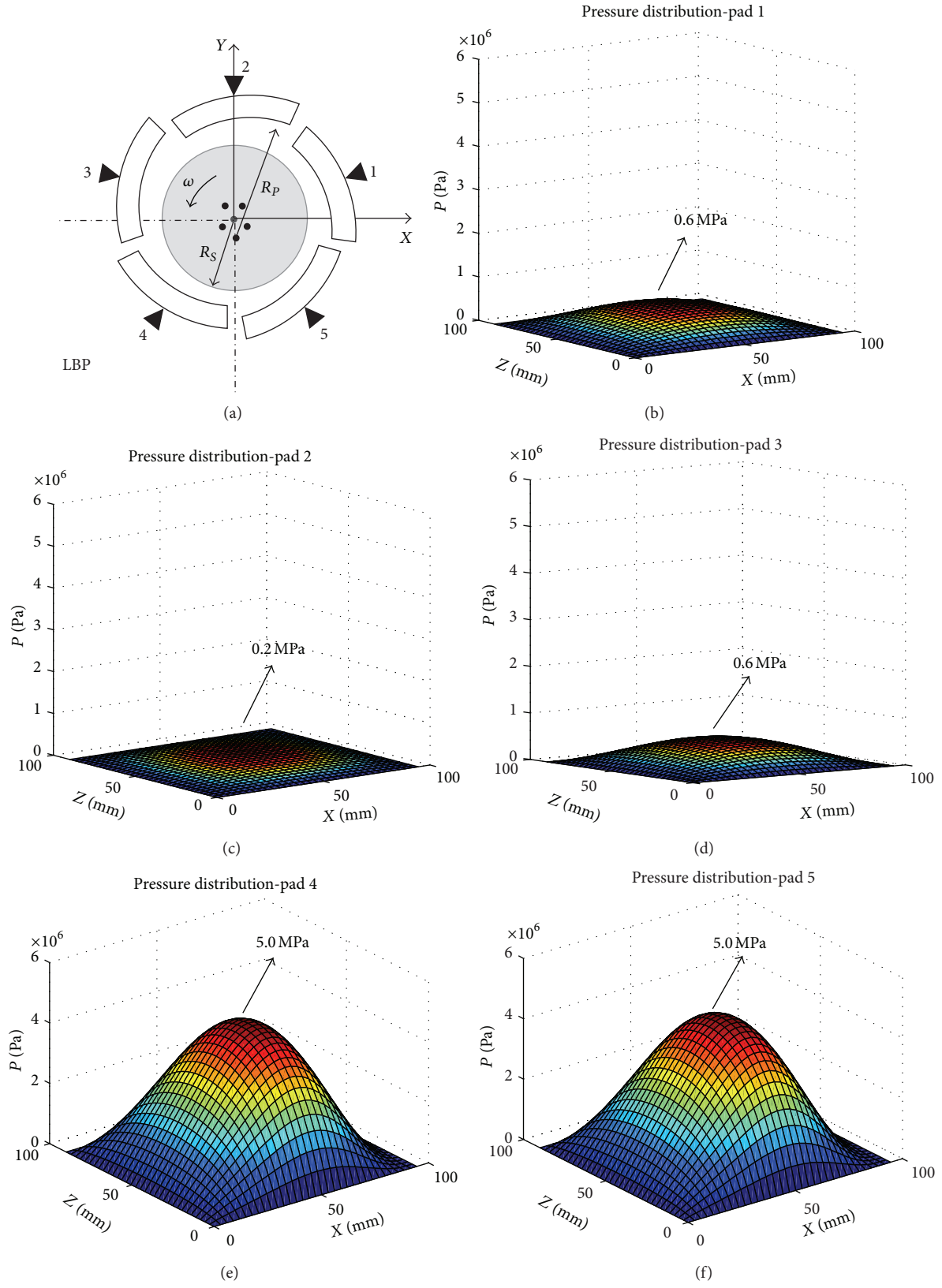

FIGURE 14: Pressure distribution on the pads obtained from the greater radial clearance and the maximum rotational speed: (a) bearing configuration; (b) pad 1; (c) pad 2; (d) pad 3; (e) pad 4; (f) pad 5.

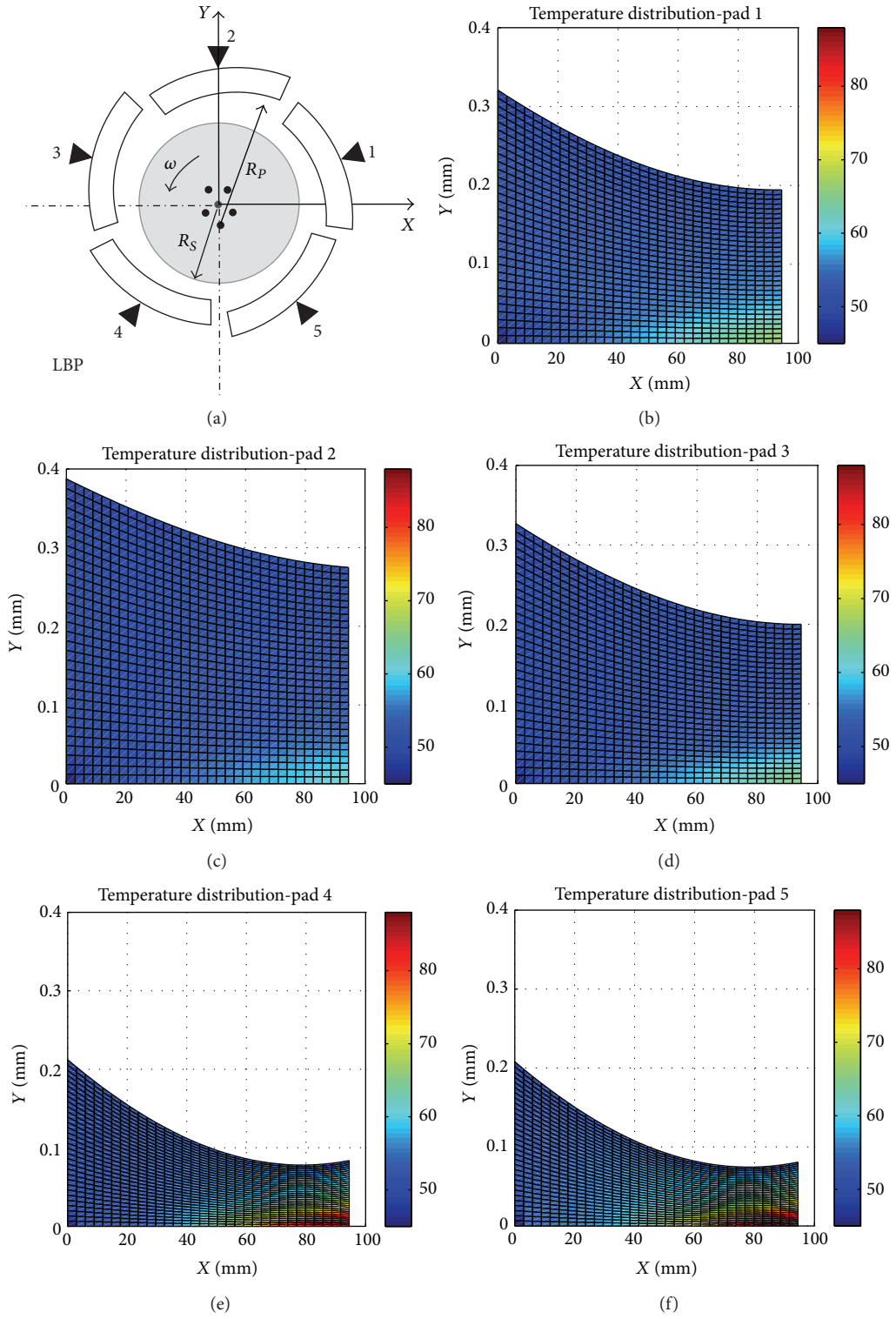

FIGURE 15: Temperature distribution on the pads obtained from the greater radial clearance and the maximum rotational speed: (a) bearing configuration; (b) pad 1; (c) pad 2; (d) pad 3; (e) pad 4; (f) pad 5.

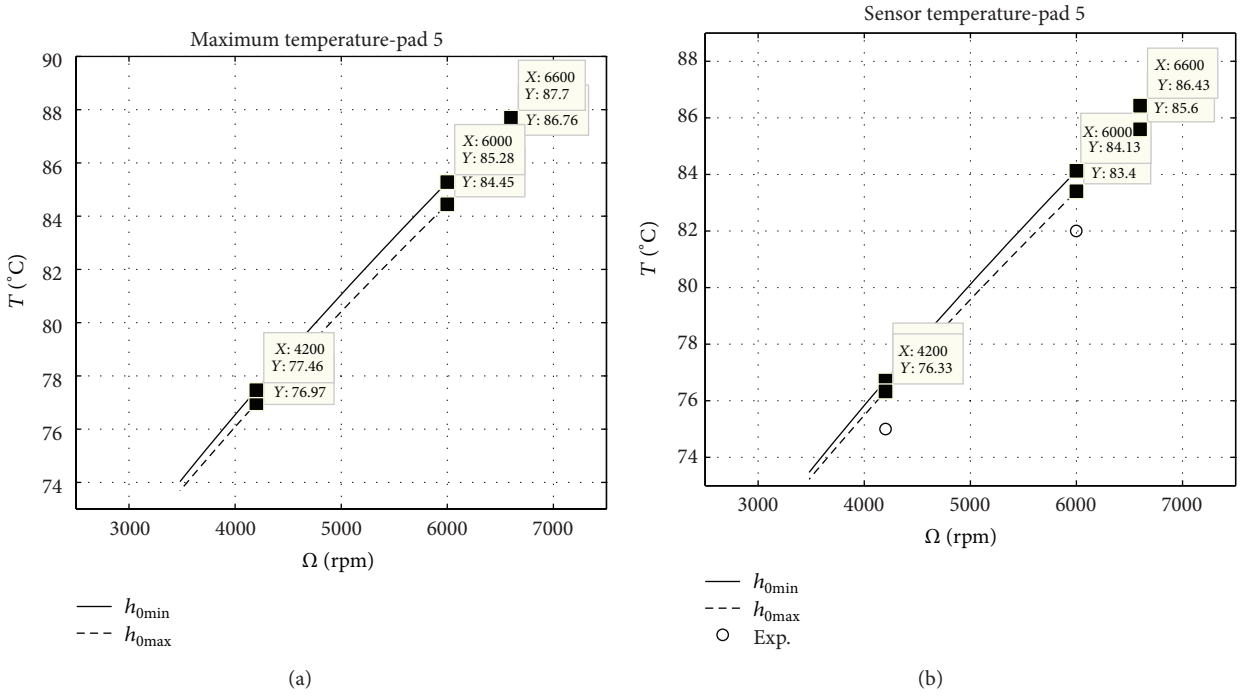

FIGURE 16: Temperature values obtained on pad 5: (a) maximum temperature; (b) temperature obtained in the sensor position.

q_O: Flow of the oil in the outlet face of a volume located at the outlet boundary of the previous pad
q_C: Flow of the oil supply (cool oil)
R_P: Radius of the pad
R_S: Radius of the shaft
T: Temperature distribution in the lubricant oil
T_C: Temperature of the oil supply (cool oil)
T_I: Temperature in the inlet face of a volume located at the inlet boundary of the next pad
T_O: Temperature in the outlet face of a volume located at the outlet boundary of the previous pad
U, u: Linear velocities filed in the X direction
V, v: Linear velocities filed in the Y direction
W, w: Linear velocities filed in the Z direction
x: Circumferential coordinate
x_S: Position of the shaft inside the bearing in the X direction
y: Radial coordinate
y_S: Position of the shaft inside the bearing in the Y direction
z: Axial coordinate
α: Angular displacement of the pad
β: Angular position on the pad
μ: Absolute viscosity of the lubricant oil
ρ: Density of the lubricant oil
Φ: Viscous dissipation of the oil.

Acknowledgments

The authors thank CNPq, CAPES-PROBRAL programme and FAPESP for the financial support of this research.

References

[1] D. Dowson, "A generalized Reynolds equation for fluid-film lubrication," *International Journal of Mechanical Sciences*, vol. 4, no. 2, pp. 159–170, 1962.

[2] D. Dowson, J. D. Hudson, B. Hunter, and C. N. March, "An experimental investigation of the thermal equilibrium of steadily loaded journal bearings," *Proceedings of the Institution of Mechanical Engineers*, vol. 181, part 3B, pp. 70–80, 1966.

[3] P. W. Hall and P. B. Neal, "The influence of film temperature boundary conditions on the performance of fluid film bearings," *International Journal of Mechanical Sciences*, vol. 17, no. 9, pp. 565–572, 1975.

[4] Y. Nagaraju, M. L. Joy, and K. Prabhakaran Nair, "Thermohydrodynamic analysis of a two-lobe journal bearing," *International Journal of Mechanical Sciences*, vol. 36, no. 3, pp. 209–217, 1994.

[5] S. Taniguchi, T. Makino, K. Takeshita, and T. Ichimura, "A thermohydrodynamic analysis of large tilting-pad journal bearing in laminar and turbulent flow regimes with mixing," *Journal of Tribology*, vol. 112, no. 3, pp. 542–548, 1990.

[6] M. Fillon, J.-C. Bligoud, and J. Frene, "Experimental study of tilting-pad journal bearings—comparison with theoretical thermoelastohydrodynamic results," *Journal of Tribology*, vol. 114, no. 3, pp. 579–588, 1992.

[7] H. C. Ha, K. W. Kim, and H. J. Kim, "Inlet pressure effects on the thermohydrodynamic performance of a large tilting pad journal bearing," *Journal of Tribology*, vol. 117, no. 1, pp. 160–165, 1995.

[8] R. K. Gadangi and A. B. Palazzolo, "Transient analysis of tilt pad journal bearings including effects of pad flexibility and fluid film temperature," *Journal of Tribology*, vol. 117, no. 2, pp. 302–307, 1995.

[9] M. Fillon and M. Khonsari, "Thermohydrodynamic design charts for tilting-pad journal bearings," *Journal of Tribology*, vol. 118, no. 1, pp. 232–238, 1996.

[10] L. Bouard, M. Fillon, and J. Frêne, "Comparison between three turbulent models—application to thermohydrodynamic performances of tilting-pad journal bearings," *Tribology International*, vol. 29, no. 1, pp. 11–18, 1996.

[11] M. Tanaka, "Recent thermohydrodynamic analyses and designs of thick-film bearings," *Journal of Engineering Tribology*, vol. 214, no. 1, pp. 107–122, 2000.

[12] Q. Chang, P. Yang, Y. Meng, and S. Wen, "Thermoelastohydrodynamic analysis of the static performance of tilting-pad journal bearings with the Newton-Raphson method," *Tribology International*, vol. 35, no. 4, pp. 225–234, 2002.

[13] P. G. Morton, "Unstable shaft vibrations arising from thermal effects due to oil shearing between stationary and rotating elements," in *Proceedings of the 9th IMechE International Conference on Vibrations in Rotating Machinery*, pp. 383–391, Exeter, UK, September 2008.

[14] K.-B. Bang, J.-H. Kim, and Y.-J. Cho, "Comparison of power loss and pad temperature for leading edge groove tilting pad journal bearings and conventional tilting pad journal bearings," *Tribology International*, vol. 43, no. 8, pp. 1287–1293, 2010.

[15] T. Dimond, A. Younan, and P. Allaire, "A review of tilting pad bearing theory," *International Journal of Rotating Machinery*, vol. 2011, Article ID 908469, 23 pages, 2011.

[16] O. Reynolds, "On the theory of lubrication and its application to Mr. Beauchamp tower's experiments, including an experimental determination of the viscosity of olive oil," *Philosophical Transactions of Royal Society of London A*, vol. 177, part 1, pp. 157–234, 1886.

[17] I. F. Santos and F. H. Russo, "Tilting-pad journal bearing with electronic radial oil injection," in *Proceedings of the ASME/STLE International Joint Tribology Conference*, San Francisco, Calif, USA, October 1996.

[18] A. Cameron, "Heat transfer in journal bearings: a preliminary investigation," in *Proceedings of the General Discussion on Heat Transfer*, pp. 194–197, Institute of Mechanical Engineers, 1951.

[19] M. He and P. E. Allaire, "Thermoelastohydrodynamic analysis of journal bearings with 2D generalized energy equation," in *Proceedings of the 6th IFToMM International Conference on Rotor Dynamics*, vol. 1, 2002.

[20] C. R. Maliska, *Transferência de Calor e Mecânica dos Fluidos Computacional*, Livros Técnicos e Científicos, Rio de Janeiro, Brazil, 2nd edition, 2004.

[21] M. K. Fitzgerald and P. B. Neal, "Temperature distributions and heat transfer in journal bearings," *Journal of Tribology*, vol. 114, no. 1, pp. 122–130, 1992.

[22] I. F. Santos and R. Nicoletti, "THD analysis in tilting-pad journal bearings using multiple orifice hybrid lubrication," *Journal of Tribology*, vol. 121, no. 4, pp. 892–900, 1999.